Defect detection method of product appearance design based on visual communication model

Tiesheng Liu

Hunan City University,
YiYang 413000, China
Email: tieshengl@mls.sinanet.com

Abstract: In order to overcome the problems of low detection accuracy and efficiency in traditional product appearance design defect detection methods, a product appearance design defect detection method based on visual communication model was proposed. The X-ray visual inspection system is used to collect the image of product appearance design, and the method of superposition of multiple images and histogram equalisation are used to denoise and enhance the defect image of product appearance design. Gabor transform is used to extract the features of the pre-processed defect image. According to the extraction results, virtual reality (VR) reconstruction method is used to construct the visual inspection model of product appearance design defects, and the defect detection of product appearance design is realised. The simulation results show that the proposed method has better detection results and improves the detection efficiency. The shortest detection time is only 5 s.

Keywords: visual communication; appearance; modelling design; defect detection; integral projection method; Gabor transform.

Reference to this paper should be made as follows: Liu, T. (2022) 'Defect detection method of product appearance design based on visual communication model', *Int. J. Product Development*, Vol. 26, Nos. 1/2/3/4, pp.39–51.

Biographical notes: Tiesheng Liu received his master's degree in design art from Hunan Normal University in 2009. He is currently a lecturer in the Art College of Hunan City University. His research interests include art design, landscape design and folk art.

1 Introduction

With the continuous development of China's economy, the manufacturing industry is gradually rising. Now, the manufacturing industry has been greatly improved both in production and manufacturing capacity, and the appearance design of products is very important. In the process of appearance design, products will cause surface defects, which will reduce the commercial value of the manufacturing industry and bring certain losses to users. In order to improve the commercial value of manufacturing products, many businesses will strictly detect the defects of product appearance design in the process of product appearance design or when it is completed, so as to achieve the goal of zero defects. Therefore, it is very important to detect the defects of product appearance design (Krummenacher et al., 2018). The defect of product appearance design is the external defect of product appearance design, which is inconsistent with the intact

product (Hawari et al., 2018; Kramer and Groche, 2018). Therefore, most people use the manual detection method to detect the defects of product appearance design, but for the small size, grey colour difference, complex background pattern and other defects cannot be achieved by manual detection. The manual detection method not only has great limitations, but also increases the labour intensity, resulting in a substantial increase in the detection cost and large error in the detection results Therefore, it is imperative to study an intelligent defect detection method for product appearance design (Li et al., 2018). With the rapid development of computer, machine vision technology is gradually accepted by people, machine vision is through the computer to simulate human visual function, extract information from the image of objective things, and carry out information processing, complete the product appearance design defect detection. Using machine vision technology instead of manual visual inspection is an important technology that cannot be replaced by manufacturing industry (Kojima et al., 2018).

In Wang et al. (2018), a defect detection system of product appearance design is designed by using TMS320DM642. The hardware of the system is designed through the defect image encoding and decoding module, image memory module and controller module of product appearance design, and then the defect image of product appearance design is collected, the collected defect image is pre-processed, and the product appearance is analysed by morphological operation Finally, according to the hardware design and software design, the detection design of product appearance design defects is completed. The simulation results show that the method can accurately detect the product appearance design defects. In Gao (2018), Canny operator edge detection method is used to study the defect detection of product appearance design. Firstly, the defect image of product appearance design is collected by CCD industrial camera, and then the minimum error segmentation method is used to identify the collected defect image of product appearance design. Finally, Canny operator edge detection method is used to complete the defect detection of product appearance design testing. Although the above two methods can accurately detect the defects of product appearance design, the detection time is longer, resulting in low detection efficiency. In Wu and Shi (2020), a method for detecting periodic defects on the surface of strip steel based on twin network is proposed. Firstly, starting from the causes of periodic defects, three main characteristics of periodic defects are summarised, namely, consistency of transverse position, similarity of defect image and unity of defect period. Then, an image similarity detection method based on twin network is proposed, which can realise periodic defects through three points Finally, the best period of the defect is fitted by the equidistance difference method, and the fitting accuracy can reach ±10 mm. In Zhou and Zhang (2020), the ultrasonic TOFD detection method for near surface defects of butt weld is proposed to accurately locate the defect position, carry out the research of image processing related technology, complete image denoising and straight through wave straightening, on this basis, the grey distribution statistical method is used to eliminate the straight through wave overlapped with the near surface defect wave, and the image segmentation algorithm is used to extract the weld defects in the ultrasonic TOFD detection image So as to realise the automatic recognition of weld defects. However, the accuracy of the above two detection methods for product appearance design defect detection is low, resulting in inaccurate detection results.

Aiming at the problems of the above methods, this paper proposes a defect detection method of product appearance design based on visual communication model:

1 Firstly, the defect image of product appearance design is collected by X-ray visual inspection system, and the obtained defect image is pre-processed.

2 According to the above pre-processing results, Gabor transform is used to extract the defect image features, and virtual reality reconstruction method is used to complete the visual inspection of product appearance design defects, which lays the foundation for improving the quality of product appearance design.

3 Experimental verification, design the comparative experiment under three indicators, and compare the proposed method with the traditional method.

2 Defect detection method of product appearance design based on visual communication model

2.1 Defect image acquisition of product appearance design

2.1.1 Image collection of product appearance design

Before the defect detection of product appearance design, the image of product appearance design is collected by X-ray visual inspection system. The principle block diagram of image acquisition by visual inspection is shown in Figure 1.

Figure 1 Schematic diagram of image acquisition by visual inspection

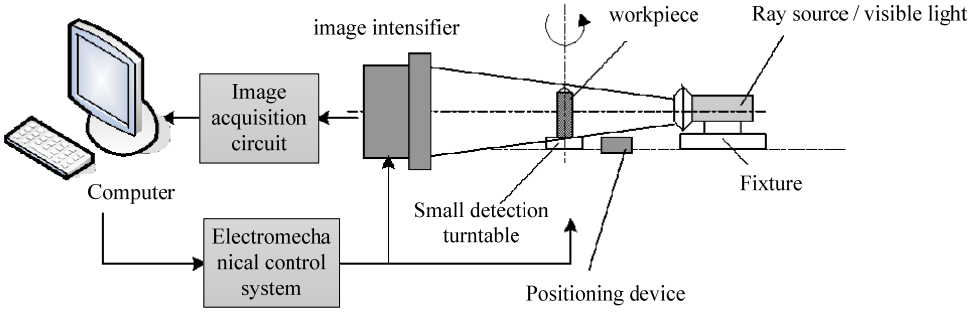

According to the principle block diagram of the image obtained by visual inspection, the product is placed on the inspection turntable, and the X-ray emitted by the ray source is used to scan the product appearance design defects in 360° to form a ray image, and then a ray is obtained every n° step. Image, all radiographic images are transferred to the computer to form an $N = 360/n$ image sequence to complete the radiographic image collection of the product appearance design (Qiu and Lau, 2018; Yao and Gu, 2018). The product appearance design image collected by the X-ray vision inspection system is shown in Figure 2.

Figure 2 The captured image

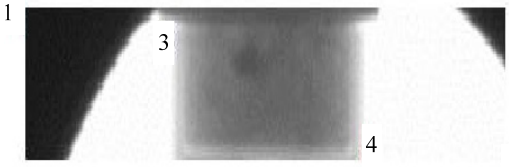

2.1.2 Determination of defect image range

In order to improve the accuracy of product appearance design defect detection, the above-mentioned collected images are used to locate product appearance design defects. The integral projection method analyses the appearance image of the product according to the projection distribution characteristics, obtains the $A \times B$ size image and the $a \times b$ size target image through the X-ray vision inspection system, and marks the coordinate positions, as shown in Figure 2, positions 3 and 4. Therefore, this paper uses the integral projection method to locate the product appearance design defects and determine the defect location (Egarguin et al., 2020).

Using formula (1) for vertical average projection, the horizontal area of the target image can be obtained:

$$V(x) = \frac{1}{y_2 - y_1} \sum_{y=y_1}^{y_2} I(x, y), (x_1 \le x < x_2) \tag{1}$$

In the formula, (x, y) represents the position of the pixel, and $I(x, y)$ represents the grey value of the pixel (Bowoto et al., 2020; Deif and Daneshmand, 2020). Similarly, the vertical area of the target image can be obtained by horizontal and vertical projection, and the expression is:

$$V(y) = \frac{1}{x_2 - x_1} \sum_{x=x_1}^{x_2} I(x, y), (y_1 \le y < y_2) \tag{2}$$

The image collected by the system is horizontal and vertical, and the curve after projection is shown in Figure 3.

Figure 3 The integral projection curve of the image

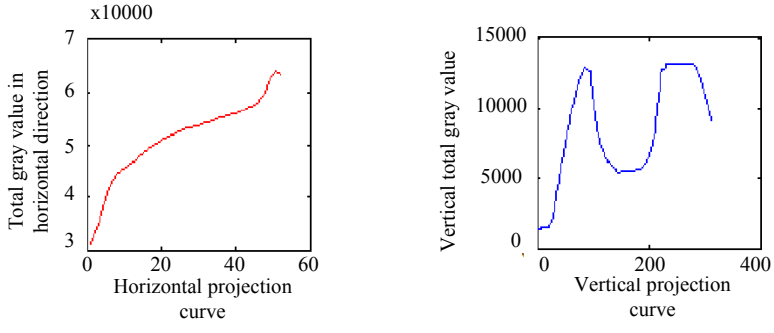

It can be seen from the integral projection curve of the image that the pixel range of the horizontal projection area is within 20–50 grey values, the grey value slope is small, and the curve changes slowly, then this area is the product appearance design defect image area. The pixel range of the vertical projection area is within the grey value of 0~90, 110~210 and 210~400. Within the grey value of 110~210, the gradient of the grey value is small and the curve change is relatively stable. This area can be judged. Design the defect image area for the appearance of the product, and the value is higher in the grey value of 0~90 and 210~400, which belongs to the invalid area. Therefore, this paper can determine whether the area is a defect image area of product appearance design through horizontal projection and vertical projection, thus narrowing the scope of judgment (Zhou et al., 2019).

After determining the position of the product appearance design defect, the defect category can be obtained. The appearance design defect of the product will be caused by the process of sintering and handling during the appearance design process. Table 1 shows the product appearance design defect classification and image examples. Among them, the red wire frame represents the defect target.

Table 1 Product appearance design defect classification and image examples

Defect type	*Image examples*	*Defect type*	*Image examples*	*Defect type*	*Image examples*
Gap	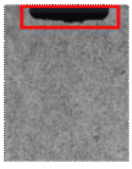	Sticky material	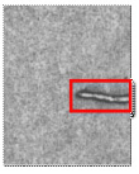	Blistering	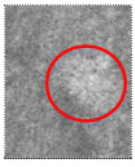
Scratch	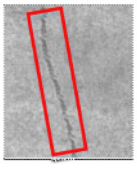	Indentation	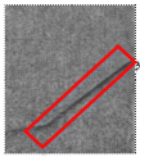	Crack	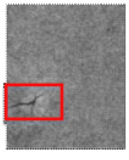

2.2 Defect image pre-processing

2.2.1 Denoising processing

When collecting images of product appearance design defects, noise will appear, which will affect the quality of the images and lead to the accuracy of product appearance design defects detection (Akram et al., 2019; Li et al., 2019). Therefore, it is necessary to denoise the collected product appearance design defect images to lay the foundation for the subsequent accurate detection of product appearance design defects. The mathematical expression of the defect image of product appearance design with noise is:

$$g(x,y) = f(x,y)V(x) + n(x,y)V(y) \tag{3}$$

In the formula, $f(x, y)$ is an ideal image without noise, $n(x, y)$ is noise, and $g(x, y)$ is an image with noise.

For the X-ray images obtained by the imaging system, the multiple image superposition method is used to denoise the product appearance design defect images. The multiple image superposition method refers to the repeated collection of product appearance design defect images and multiple collections The image of is superimposed and averaged to denoise the image. The expression is:

$$h(x,y) = g(x,y) f(x-t, y-l), (t,l \in T) \tag{4}$$

In the formula, $h(x, y)$ is the image after filtering and denoising, $f(x - t, y - 1)$ is the grey value corresponding to each pixel in the original image in the sliding window, and T is the sliding window. The size of the window is agreed to be an odd number.

2.2.2 Enhanced processing

The product appearance design defect image will be disturbed when it is collected, resulting in weakening of image characteristics, and inconsistency with the actual product appearance design defect image, resulting in reduced accuracy when detecting product appearance design defects, and the detection effect is not ideal In order to improve the image quality of product design defects, make the images clearer, show more comprehensive and useful image information, and improve the machine's ability to detect images, this article uses histogram equalisation to balance the collected product appearance design defects The image is enhanced (Roy et al., 2019; Chou et al., 2019).

Histogram equalisation is an image enhancement method. By establishing a mathematical model of histogram equalisation, the grey-scale histogram of the product appearance design defect image becomes smooth, and the processed product appearance design defect image is replaced by the collection The original image of the product, thereby enhancing the product appearance design defect detection capabilities.

Assuming that the grey level of the defect image of the discretised product design can be expressed as r_i ($i = 0, 1, \ldots, L - 1$, L is the number of grey levels), the expression of the grey level probability $p(r_i)$ of the defect image of the discretised product design is:

$$p(r_i) = \frac{n_i}{N} h(x,y) \tag{5}$$

In the formula, N represents the total number of defective image pixels of the product appearance design, and n_i represents the number of occurrences of the i-th grey level r_i. The transformation function for histogram equalisation of the product appearance design defect image:

$$s_i = R(r_i) = \sum_{i=0}^{L-1} p(r_i) = \sum_{i=0}^{L-1} \frac{n_i}{N} \tag{6}$$

The inverse transform function of histogram equalisation on the product appearance design defect image:

$$r_i = T^{-1}(s_i) \tag{7}$$

2.3 Feature extraction of appearance design defects

In order to improve the accuracy, robustness and scalability of the algorithm, texture feature extraction is performed on the pre-processed product appearance design defects. The texture feature is to transform the product design defect image, extract the feature value in the defect image, and the feature value represents the consistency and difference in the product design defect image area. In this paper, Gabor transform is used to extract the features of product appearance design defects. According to the nature of convolution, the Fourier transform of the impulse response of the Gabor filter is the convolution of the Fourier transform of its harmonic function and the Fourier transform of the Gaussian function. The filter consists of an imaginary part and a real part, which are orthogonal to each other. A set of Gabor functions with different wavelengths and different directions is very effective for texture feature extraction.

The mathematical expression of Gabor function for product appearance design defect feature extraction is as follows:

$$g\left(x,y;\tau,\varphi,\sigma,\gamma\right)=\exp\left(-\frac{x'^2+\gamma y'^2}{2\sigma^2}\right)\exp\left[i\left(2\pi\frac{x'}{\tau}\right)+\varphi r_i\right] \tag{8}$$

The real part and imaginary part are:

$$g\left(x,y;\tau,\varphi,\sigma,\gamma\right)=\exp\left(-\frac{x'^2+\gamma y'^2}{2\sigma^2}\right)\cos\left(2\pi\frac{xx'}{\tau}+\varphi r_i\right) \tag{9}$$

$$g\left(x,y;\tau,\varphi,\sigma,\gamma\right)=\exp\left(-\frac{x'^2+\gamma y'^2}{2\sigma^2}\right)\sin\left(2\pi\frac{x'}{\tau}+\varphi r_i\right) \tag{10}$$

Among them:

$$x'=x\cos\theta+y\sin\theta \tag{11}$$

$$y'=-x\sin\theta+y\cos\theta \tag{12}$$

In the formula, wavelength τ, direction θ, phase shift φ, aspect ratio γ, and bandwidth b are all Gabor filter parameters.

2.4 Visual inspection model for product appearance design defects

The wavelet function $R(x, y)$ of eigen-decomposition is:

$$R\left(x,y\right)=x^2+y^2+wx+ky \tag{13}$$

In the formula, w and k respectively represent the prior information and the correlation coefficient of the visual feature reconstruction of product appearance design defects.

In the maximum search area, the VR virtual reality reconstruction method is used to construct a visual inspection model for product appearance design defects, and the expression is:

$$J(t)=R\left(x,y\right)(\delta x+\varepsilon y)^2t \tag{14}$$

According to the product appearance design defect feature extraction results, the edge scale entropy of product appearance design defect feature calibration on each scale $\mu(n)$ is obtained. Using the distribution strength of edge scale entropy, the product appearance design defect feature calibration points are sorted. Through the sorting results, the visual information of product appearance design defect is decomposed to complete the product design The construction of visual inspection model of appearance design defects.

3 Simulation experiment analysis

To verify the appearance of the product design model based on the performance of visual communication defect detection method in practical applications, in MATLAB simulation software, to conduct a simulation by-line detection system. Figure 4 shows the online inspection system for product appearance design defects.

Figure 4 Online detection system

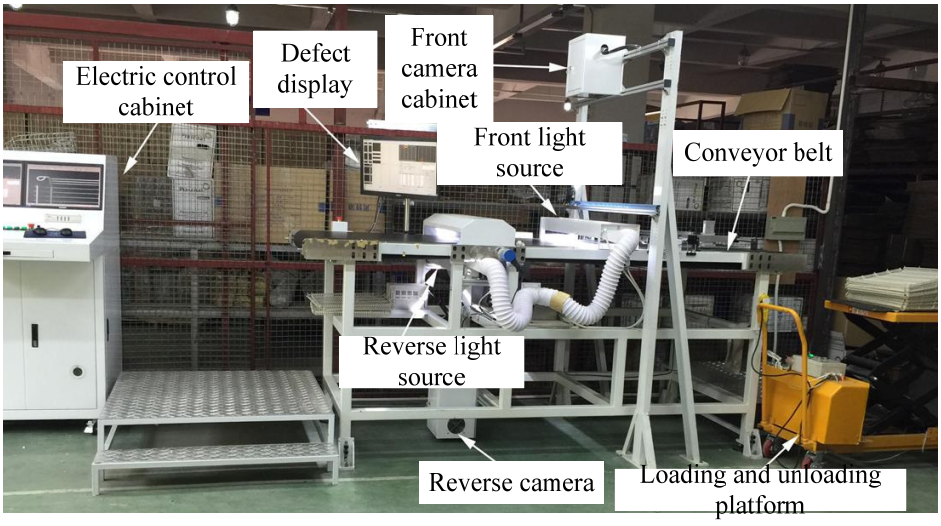

In this paper, metal workpiece products are used as experimental objects to detect defects in the appearance design of metal workpiece products. The image of the metal workpiece product is collected by the X-ray vision inspection system, as shown in Figure 5.

Pre-process the acquired image samples, and the product effect diagram after pre-processing is shown in Figure 6.

Under the above conditions, the overall experimental scheme is set as follows: Taking the defect detection results, defect accuracy and defect detection time as the experimental comparison indexes, the method in this paper is compared with the methods in Gao (2018) and Wu and Shi (2020).

Figure 5 Original image of metal workpiece

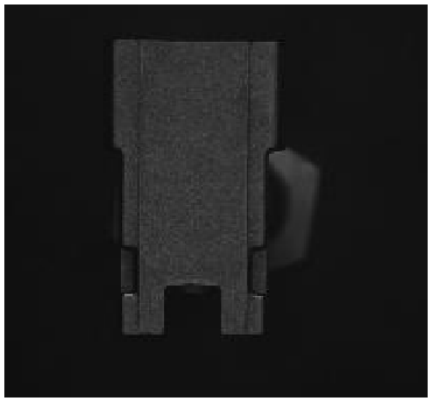

Figure 6 Product rendering after pre-treatment

3.1 Comparison of defect detection results

After the pre-treatment of the metal workpiece product, the product appearance design defect detection method based on the visual communication model proposed in this paper, the machine learning-based product appearance design defect detection method proposed in Gao (2018) and the twin based on Wu and Shi (2020). The web-based product appearance design defect detection method detects defects in the appearance design of metal workpieces. The detection results of the product appearance design defects are shown in Table 2.

Analysis of the defect images in Table 2 shows that the product appearance design defect detection method based on the visual communication model proposed in this paper can accurately detect the appearance design defects of metal workpieces. However, the method of Gao (2018) and Wu and Shi (2020) metal workpiece product appearance design defect detection results are inaccurate, indicating that the product appearance design defect detection effect in this article is better.

Table 2 Defect detection results of product appearance design

	Gap	*Sticky material*	*Indentation*	*Crack*	*Scratch*	*Blistering*
Defect sample	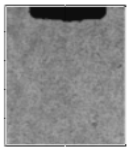	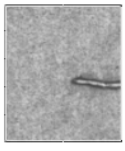	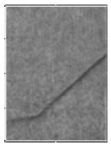	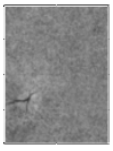	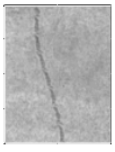	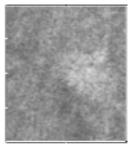
Gao (2018) method				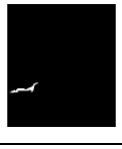		
Wu and Shi (2020) method			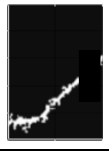		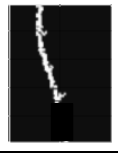	
Method of this article			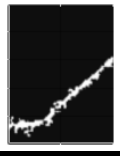		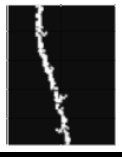	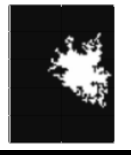

3.2 Comparison of detection accuracy

In order to verify the effectiveness of the method in this paper, the product appearance design defect detection method based on the visual communication model proposed in this paper, the machine learning-based product appearance design defect detection method proposed in Gao (2018) and the product appearance design defect detection method based on Wu and Shi (2020). The product appearance design defect detection accuracy of the product appearance design defect detection method of Twins Network is compared and analysed, and the comparison results are shown in Table 3.

Table 3 Comparison of detection accuracy of product appearance design defects/%

Number of experiments	*Method of this article*	*Gao (2018) method*	*Wu and Shi (2020) method*
10	92.6	73.5	51.3
20	92.9	74.1	52.6
30	93.2	76.1	53.4
40	94.8	77.3	53.8
50	95.2	78.2	54.2
60	95.6	79.4	55.6
70	96.7	80.1	56.7
80	97.6	82.5	57.2
90	98.2	83.1	58.4
100	99.9	85.6	59.4

According to the data in Table 3, with the increase of the number of experiments, the detection accuracy of product appearance design defects in this method, Gao (2018) method and Wu and Shi (2020) is gradually increasing, and the detection accuracy of this method can reach 99.9%, while the detection accuracy of Gao (2018) method and Wu and Shi (2020) method is only 85.6% and 59.4%. The detection accuracy of this method is higher than that of traditional methods.

3.3 Comparison of detection time

In order to verify the effectiveness of the method, the method herein, Gao (2018) and the method of Wu and Shi (2020), product appearance design accuracy of defect detection were analysed, comparing the results obtained which are shown in Figure 7.

Figure 7 Comparison of detection time

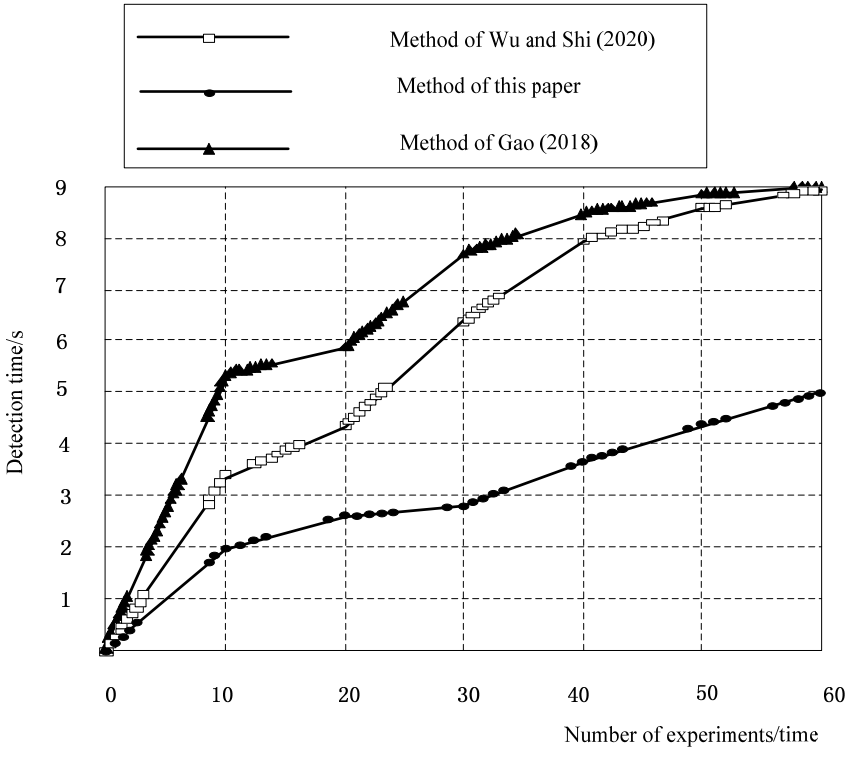

According to Figure 7, the product appearance design defect detection time of the method in this paper is within 5 s, while the product appearance design defect detection time of Gao (2018) method and Wu and Shi (2020) method is within 9 s. The product appearance design of the method in this paper. The defect detection time is shorter than that of Gao (2018) method and the product appearance design defect detection time of Wu and Shi (2020) method.

4 Conclusion

In order to improve the quality of product appearance design, it is necessary to study on-line adaptive automatic non-destructive testing method. In this paper, a new defect detection method of product appearance design based on visual communication model is proposed, and the performance of the method is verified theoretically and experimentally. This method has high detection accuracy and low detection time, the highest detection accuracy can reach 99.9%, and the shortest detection time is only 5 s. It not only ensures the quality of product appearance design defect detection, but also improves the speed of product appearance design defect detection, which lays the foundation for manufacturing production and processing.

References

Akram, M.W., Li, G., Jin, Y., Chen, X., Zhu, C., Zhao, X., Aleem, M. and Ahmad, A. (2019) 'Improved outdoor thermography and processing of infrared images for defect detection in PV modules', *Solar Energy*, Vol. 19, No. 10, pp.549–560.

Bowoto, O.K., Oladapo, B.I., Zahedi, S.A., Omigbodun, F.T. and Emenuvwe, O.P. (2020) 'Analytical modelling of in situ layer-wise defect detection in 3D-printed parts: additive manufacturing', *The International Journal of Advanced Manufacturing Technology*, Vol. 11, No. 7, pp.1–11.

Chou, Y.C., Liao, W.C., Chen, Y.L., Chang, M. and Lin, P.T. (2019) 'A distributed heterogeneous inspection system for high performance in-line surface defect detection', *Intelligent Automation & Soft Computing*, Vol. 25, No. 1, pp.79–90.

Deif, S. and Daneshmand, M. (2020) 'Multiresonant chipless RFID array system for coating defect detection and corrosion prediction', *IEEE Transactions on Industrial Electronics*, Vol. 67, No. 10, pp.8868–8877.

Egarguin, N.J.A., Meklachi, T., Onofrei, D. and Harari-Arnold, N.D. (2020) 'Vibration suppression and defect detection schemes in 1D linear spring-mass systems', *Journal of Vibration Engineering & Technologies*, Vol. 33, No. 12, pp.1–15.

Gao, N. (2018) 'Design and simulation of bearing appearance defect detection algorithm', *Computer and Digital Engineering*, Vol. 46, No. 11, pp.188–191.

Hawari, A., Alamin, M., Alkadour, F., Elmasry, M. and Zayed, T. (2018) 'Automated defect detection tool for closed circuit television (cctv) inspected sewer pipelines', *Automation in Construction*, Vol. 89, No. 25, pp.99–109.

Kojima, N., Taketani, Y., Morita M., et al. (2018) 'Method of defect detection in PEFCs using magnetic sensor', *ECS Transactions*, Vol. 83, No. 1, pp.1–11.

Kramer, P. and Groche, P. (2018) 'Defect detection in thread rolling processes – experimental study and numerical investigation of driving parameters', *International Journal of Machine Tools & Manufacture*, Vol. 12, No. 5, pp.27–36.

Krummenacher, G., Ong, C.S., Koller, S., Kobayashi, S. and Buhmann, J.M. (2018) 'Wheel defect detection with machine learning', *IEEE Transactions on Intelligent Transportation Systems*, Vol. 9, No. 4, pp.1176–1187.

Li, C., Liu, C., Gao, G., Liu, Z. and Wang, Y. (2019) 'Robust low-rank decomposition of multi-channel feature matrices for fabric defect detection', *Multimedia Tools & Applications*, Vol. 78, No. 6, pp.7321–7339.

Li, R., Yuan, Y., Zhang, W. and Yuan Y. (2018) 'Unified vision-based methodology for simultaneous concrete defect detection and geolocalization', *Computer□aided Civil & Infrastructure Engineering*, Vol. 33, No. 7, pp.527–544.

Qiu, Q. and Lau, D. (2018) 'Defect detection in FRP-bonded structural system via phase-based motion magnification technique', *Structural Control and Health Monitoring*, Vol. 25, No. 12, pp.2259–2266.

Roy, D., Babu, P. and Tuli, S. (2019) 'Sparse reconstruction-based thermal imaging for defect detection', *IEEE Transactions on Instrumentation and Measurement*, Vol. 13, No. 7, pp.1–9.

Wang, H., Hao, L., Yang, J. and Li, S. (2018) 'Design and realization of bearing defect inspection system', *Modern Manufacturing Engineering*, Vol. 45, No. 5, pp.156–161.

Wu, K. and Shi, J. (2020) 'Method for detecting periodic defects on strip surface based on twin network', *Metallurgical Automation*, Vol. 65, No. 6, pp.97–102.

Yao, M. and Gu, Q. (2018) 'A sparse representation method for image-based surface defect detection', *Optoelectronics Letters*, Vol. 14, No. 6, pp.82–86.

Yu, Q., Obeidat, O. and Han, X. (2018) 'Ultrasound wave excitation in thermal NDE for defect detection', *NDT & E International*, Vol. 10, No. 8, pp.153–165.

Zhou, H. and Zhang, X. (2020) 'Research on automatic identification method of ultrasonic TOFD inspection for butt welds near surface defects', *Journal of Lishui University*, Vol. 23, No. 5, pp.89–95.

Zhou, Z., Wang, C., Gao, X., Zhu, Z., Hui, X., Zheng, X. and Jiang, L. (2019) 'Fabric defect detection and classifier via multi-scale dictionary learning and an adaptive differential evolution optimized regularization extreme learning machine', *Fibres & Textiles in Eastern Europe*, Vol. 27, No. 1, pp.67–77.